JAASCI http://jaasci.com
JOURNAL OF ADVANCED APPLIED SCIENCES
e-ISSN: 2979-9759
PRENSIP https://prensip.gen.tr

RESEARCH ARTICLE

Influence of Mg, Sr, TiB, and Cu Additions on the Microstructure and Mechanical Behavior of A356 Alloy Wheels

Ezgi Zengin[1]✉ • Parvina Irgasheva[2]

[1]Dokuz Eylül University, Faculty of Engineering, Department of Materials Science and Engineering, İzmir/Türkiye
[2]Middle East Technical University, Faculty of Engineering, Department of Metallurgical and Materials Engineering, Ankara/Türkiye

ARTICLE INFO

Article History
Received: 01.10.2025
Accepted: 02.12.2025
First Published: 31.12.2025

Keywords
A356 alloy
Alloying elements
Mechanical properties
Microstructure

ABSTRACT

This research investigates the influence of magnesium (Mg), strontium (Sr), titanium boride (TiB), and copper (Cu) additions on the mechanical and microstructural behavior of A356 aluminum alloy wheel components produced by low-pressure casting and subjected to T6 heat treatment. Tensile and hardness tests were performed across three critical wheel regions to evaluate localized performance variations caused by casting conditions. Results demonstrate that increasing Mg content from 0.05 wt.% to 0.15 wt.% leads to a measurable decrease in ductility, with elongation reductions of 0.3–0.7% depending on the region, while simultaneously increasing hardness through Mg_2Si precipitation strengthening. Sr additions at realistic modification levels (0.005–0.015 wt.%) produced a clear transition of eutectic Si from acicular to spheroidized morphology, improving yield strength by approximately 15–20 MPa, particularly in the inner flange. Copper additions enhanced tensile and yield strength through precipitation hardening, although excessive Cu levels reduced ductility due to the presence of coarse intermetallic phases. Overall, the findings demonstrate that controlled additions of Mg, Sr, TiB, and Cu significantly influence the regional mechanical response of A356 alloy wheels. The study highlights the importance of localized microstructural analysis for optimizing alloy design and improving casting performance.

Please cite this paper as follows:
Zengin, E., & Irgasheva, P. (2025). Influence of Mg, Sr, TiB, and Cu additions on the microstructure and mechanical behavior of A356 alloy wheels. *Journal of Advanced Applied Sciences*, *4*(1-2), 37-44. https://doi.org/10.61326/jaasci.v4i1-2.420

1. Introduction

Many structural elements in the automotive and aviation sectors have a growing dependence on aluminum alloys due to their great wear resistance, low cost, and high power-to-weight ratio (Stojanovic et al., 2018). For the automotive and aviation industries, fuel consumption and performance are affected by weight, as more weight results in higher fuel consumption and lower performance (Musfirah & Jaharah, 2012). Aluminum alloy wheels are critical structural components in the automotive industry, offering a balance between mechanical strength and weight optimization. An aluminum-silicon alloy, A356, has been extensively used in the automotive industry because of its excellent casting characteristics and corrosion resistance (Aguirre-De la Torre et al., 2013). The A356 alloy is widely used in a number of applications for structural components of an automobile, such as alloy wheels, supporting brackets, and housing, through various casting processes (Do Lee, 2007). Moreover, additional alloying elements can be used to further improve the strength of these alloys (Pramod et al., 2019). Recent studies have shown that tailored alloying

✉ Correspondence
E-mail address: ezgi.zengin@renault.com

strategies and advanced grain refiners can further enhance both strength and ductility, especially when using optimized Ti- and Sr-based additions (Xu et al., 2024; S. Zhang et al., 2023). The mechanical properties of cast Al-Si-based alloys commonly used in wheel manufacturing are highly sensitive to factors such as chemical composition, solidification behavior, and microstructural evolution (Tash et al., 2006).

The size and shape of grains, dendrite arm spacing (DAS), and the size and distribution of secondary phases are critical microstructural features that influence the mechanical behavior of cast components (Kori et al., 2000). Refining these features leads to significant improvements in mechanical performance. In A356 alloy, controlling and reducing DAS is particularly effective: as DAS decreases, porosity diminishes and second-phase particles become more uniformly dispersed, resulting in enhanced mechanical properties (Gandin, 2000; Gowri & Samuel, 1994; Kashyap et al., 1993; Shabestari & Moemeni, 2004; Veldman et al., 2001; Wang & Davidson, 2001). Recent investigations into heat-treatment regimes further emphasize the strong link between microstructural refinement and mechanical performance improvements in A356 alloys (Nnakwo et al., 2024).

In the A356 alloy, the primary factors affecting mechanical properties include the types of intermetallic compounds such as iron and copper, the size and distribution of porosity, the morphology and size of eutectic silicon particles, and the solubility levels of Mg and Cu elements in the α-Al matrix after solution strengthening (Wang & Davidson, 2001). The addition of Sr to an A356 alloy further improves the mechanical qualities of the A356 alloy, such as higher tensile strength and elongation (Yan et al., 2021). Similarly, the addition of TiB_2—introduced via Al-5Ti-1B superalloy—creates new nucleation sites in the A356 alloy, which catalyzes significant grain refinement and subsequently an increase in tensile strength, yield strength, and ductility (Chowwanonthapunya & Peeratatsuwan, 2019). Wear resistance is also a critical feature of the A356 alloy. Several studies have demonstrated that copper (Cu) additions significantly improve the wear resistance of the alloy (Colak et al., 2016; Kashimat et al., 2023). More recent work confirms that Cu additions between 1–4 wt% can substantially enhance wear resistance and hardness, particularly after heat treatment, though excessive copper can induce embrittlement (Deepak et al., 2025).

The current literature studies regarding this topic include the influence of alloying elements such as Si, Mg, Cu, and TiB on microstructure; however, they consider the wheel structure as a homogeneous component. This approach fails to consider heterogeneous regions that arise due to the complex geometry of the wheel. Current automotive wheels are composed of numerous geometrically distinct regions, namely the hub, spokes, and rim. These geometrical distinctions affect the design parameters, as well as wall thickness and manufacturing constraints, which result in variability of local solidification rates, thermal gradients, and melt flow directions during casting. Inevitably, these variables affect key microstructural properties such as DAS, porosity distribution, elemental segregation, and precipitation kinetics.

Given these gaps, the following question comes to mind: how do the geometrically distinct regions of an A356 aluminum wheel respond, both microstructurally and mechanically, to TiB addition under industrial low-pressure casting conditions?

In this study, we investigate the local mechanical behavior of different regions of cast aluminum wheels through experimental procedures including hardness measurements, elongation tests, and microstructural investigation. Rather than assuming material homogeneity throughout the entirety of aluminum wheels, this work provides a region-specific perspective by investigating the microstructural and mechanical variations induced by both geometry and TiB addition.

2. Materials and Methods

This study investigates the influence of selected alloying elements on the mechanical properties of aluminum wheels manufactured using A356 alloy via casting. The measurements of the manufactured wheels are 7Jx17. All samples were produced using the low-pressure die casting method with a designated mold. Commercially available A356 aluminum alloy ingots served as the base material. To ensure metal cleanliness, all specimens were subjected to a standard degassing procedure following the melting process. Table 1 presents the chemical composition of the A356 alloy used as the base material.

Table 1. Chemical composition of the A356 aluminum alloy, showing the weight percentage (wt.%) of major and minor alloying elements.

Element	Si	Mg	Cu	Fe	Sr	Ti
Balance	7	0.3	0.02	0.15	0.01	0.03

All samples were produced using the low-pressure casting method with a designated mold. After melting, the commercial A356 alloy underwent standard degassing procedures. Subsequently, alloying elements were added to the molten metal in predetermined proportions. The samples intended for heat treatment underwent a T6 heat treatment process, comprising solution treatment at 540 °C for 4 hours, followed by quenching in water and artificial aging at 150 °C for 4 hours. During wheel production, machining and painting processes were applied. It is essential to consider that the elevated temperatures encountered during the painting process may induce secondary aging effects. This may slightly alter the mechanical properties post-T6 treatment. Nonetheless, all specimens were subjected to identical processing conditions to ensure consistency and reliability in the comparative analysis.

Tensile tests were performed using a Zwick Z100 universal testing machine to evaluate the yield strength, ultimate tensile strength, and elongation of the samples. Test specimens were prepared in accordance with DIN EN ISO 6892-1 standards to obtain consistent and reliable results. Mechanical tests were performed on three critical regions of the sample wheels, as shown in Figure 1. To ensure the reliability of the results, each region was tested three times, and the mean values were used to plot the graphs. Region 1 represents the inner flange, Region 2 represents the outer flange, and lastly, Region 3 represents the spoke region.

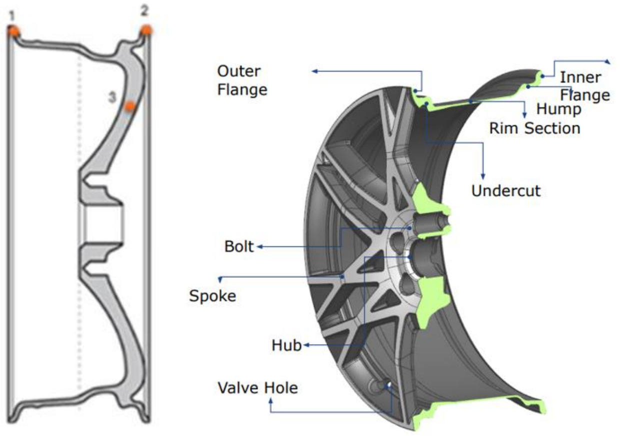

Figure 1. Selected regions of the A356 aluminum wheel used for mechanical testing, illustrating the locations where hardness and tensile samples were collected.

- Region 1: Inner flange
- Region 2: Outer flange
- Region 3: Spoke

Hardness measurements were performed using the Brinell hardness method with the Innovatest Nemesis 9000 device. For each specimen, three hardness tests were conducted. The experimental alloy compositions utilized in this study are summarized in Table 2. A total of twelve distinct alloying compositions were systematically designed and implemented to evaluate the effects of varying element concentrations on the mechanical behavior of the A356 alloy.

Table 2. Experimental compositions of the modified A356 alloy, showing the added amounts of Mg, Sr, TiB, and Cu used in each trial (wt.%).

Material	**Property**	**Concentration (%)**	**Spoke**	**Inner Flange**	**Outer Flange**
Sr	Yield Strength (MPa)	0.05	215.00 ± 1.00	263.00 ± 1.00	265.67 ± 7.23
		0.10	228.00 ± 1.00	279.67 ± 1.53	266.33 ± 18.50
		0.15	232.00 ± 1.00	283.00 ± 1.00	274.00 ± 12.17
Mg	Hardness (HB)	0.05	71.77 ± 0.25	63.60 ± 0.30	71.77 ± 0.25
		0.10	72.20 ± 0.20	65.13 ± 0.15	72.20 ± 0.20
		0.15	74.00 ± 0.20	65.77 ± 0.25	74.00 ± 0.20
	Elongation (%)	0.05	3.37 ± 0.15	10.50 ± 0.10	9.30 ± 0.10
		0.10	3.17 ± 0.15	10.70 ± 0.10	9.00 ± 0.10
		0.15	2.97 ± 0.15	10.07 ± 0.15	8.57 ± 0.15
TiB	Hardness (HB)	0.05	73.10 ± 0.10	65.30 ± 0.10	73.20 ± 0.10
		0.10	73.60 ± 0.10	65.80 ± 0.10	73.70 ± 0.10
		0.15	74.10 ± 0.10	66.20 ± 0.10	74.17 ± 0.15

3. Results and Discussion

3.1. Effect of Mg

Figure 2(a), (b), and (c) present the tensile and hardness test results with error bars for the three critical regions with varying Mg content. An inverse relationship between Mg content and ductility is evident. Specifically, in the Spoke region, elongation decreases from 3.37% at 0.05 wt.% Mg to 2.97% at 0.15 wt.% Mg. The Inner Flange exhibits a slight increase in elongation from 0.05 wt.% to 0.10 wt.% Mg, reaching a peak of approximately 10.7%, followed by a decline to about 10.1% at 0.15 wt.% Mg. The Outer Flange shows a decreasing trend similar to the Spoke region, with elongation dropping from 9.3% at 0.05 wt.% Mg to 8.6% at 0.15 wt.% Mg.

These results indicate that increasing Mg content promotes more brittle behavior, leading to reduced ductility. Statistical analysis confirms that the observed changes in elongation are significant, with p-values < 0.05 for all regions. The percentage variation among the three repetitions per region was generally below 5%, indicating acceptable measurement reproducibility. As shown by the error bars in Figure 2, the inner and outer flanges exhibit narrower variability compared to the Spoke region, suggesting more uniform mechanical behavior in those areas despite variations in Mg content.

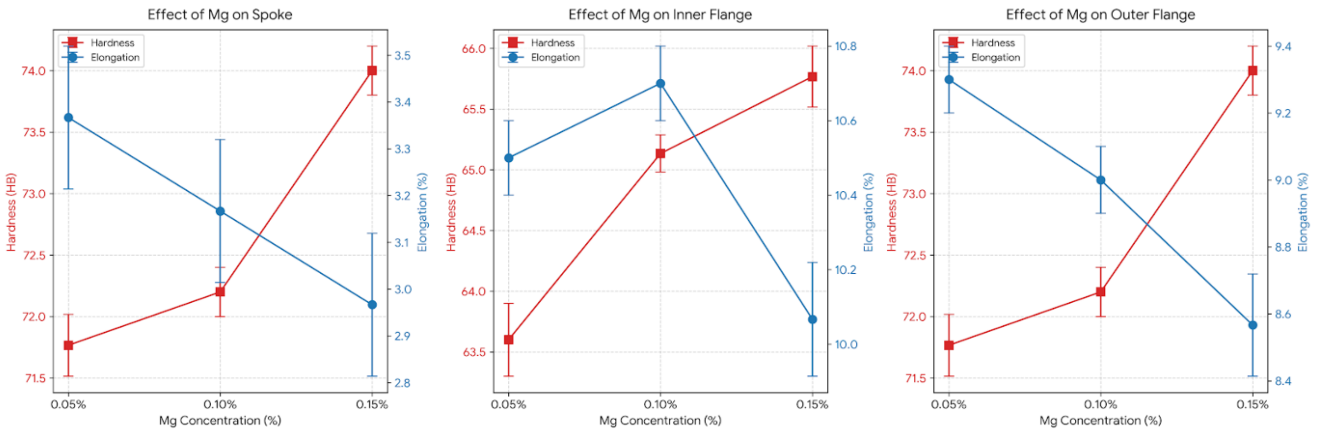

Figure 2. Effects of Varying Mg content on the elongation percentage of an A356 alloy for spoke, inner flange and outer flange.

Across all regions, Brinell hardness increases steadily as Mg rises from 0.05 wt.% to 0.15 wt.%, directly mirroring the decline in ductility observed in the same plots. The Spoke and Outer Flange regions, which are subject to higher cooling rates, exhibit higher base hardness values, peaking at 74 HB at 0.15 wt.% Mg. The Inner Flange shows a lower baseline but a similar upward trend, rising from 63.6 HB to roughly 65.8 HB.

This hardening effect is primarily due to solid solution strengthening and the formation of Mg_2Si precipitates. In dendritically solidified AlSi7 alloys, these precipitates migrate to grain boundaries, effectively hindering dislocation motion (Cáceres & Rovera, 2001). These precipitates strengthen the alpha-Al matrix via a mechanism called Orowan Looping. In this mechanism, dislocations are forced to bow around non-deformable particles rather than cutting through them (Y. Zhang & Sills, 2023). The increase in yield strength can be attributed to the increase in volume fraction of the above-mentioned precipitates. The combined graphs clearly depict the mechanical trade-off: as the precipitation hardening mechanism becomes more pronounced with higher Mg content, the material gains strength (hardness) at the expense of plastic deformation capability (elongation). The error bars for hardness are notably narrow (SD < 0.3 HB) across all trials, indicating high measurement reproducibility and a uniform response to heat treatment, despite the microstructural differences inherent to the varying geometries of the spoke and flange regions.

3.2. Effect of Sr

Microstructural differences resulting from varying strontium (Sr) additions were investigated using optical microscopy. Figure 3(a)–(b) present comparative micrographs illustrating the effect of Sr on the morphology of eutectic silicon particles.

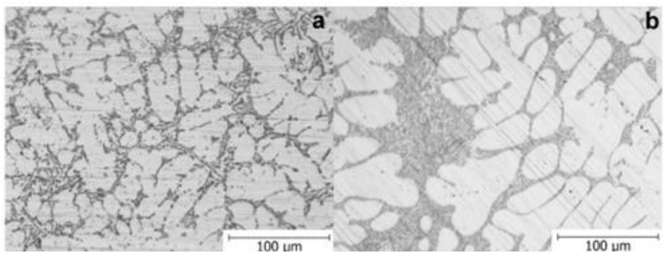

Figure 3. Micrographic images of an A356 alloy with addition of Sr as an alloying element.

In the unmodified sample (Figure 3(a)), the microstructure consists of coarse, acicular (needle-like) silicon (Si) phases. These features act as stress concentrators, negatively affecting both elongation and tensile strength. With the addition of Sr at experimental levels (0.05–0.15 wt.%), as shown in Figure 3(b)–

(c), the eutectic Si transforms into a more spheroidized morphology, indicating improved microstructural uniformity. This modification reduces stress concentration points, promoting more ductile behavior.

The effect of Sr content on the yield strength of the A356 alloy was evaluated in the three critical regions: inner flange (Region 1), outer flange (Region 2), and spoke (Region 3). The results are presented in Figure 4, where yield strength shows a gradual increase with Sr content. In the spoke region, yield strength rises from approximately 215 MPa at 0.05 wt.% Sr to around 232 MPa at 0.15 wt.% Sr. The most significant improvement occurs between 0.05 and 0.10 wt.% Sr. Similarly, the inner flange shows an increase in yield strength from roughly 263 MPa to 283 MPa over the same Sr range.

These improvements are closely linked to the spheroidization of eutectic Si particles. In unmodified alloys, the needle-like Si morphology contributes to brittleness, whereas Sr-induced spheroidization enhances ductility and mechanical integrity (Yang et al., 2023). Statistical analysis indicates that the observed increases in yield strength are significant ($p < 0.05$). The percentage variation across three repeated measurements was generally below 1% for the inner flange and spoke, confirming high reproducibility, though the outer flange exhibited higher variability (up to ~7%) at intermediate concentrations.

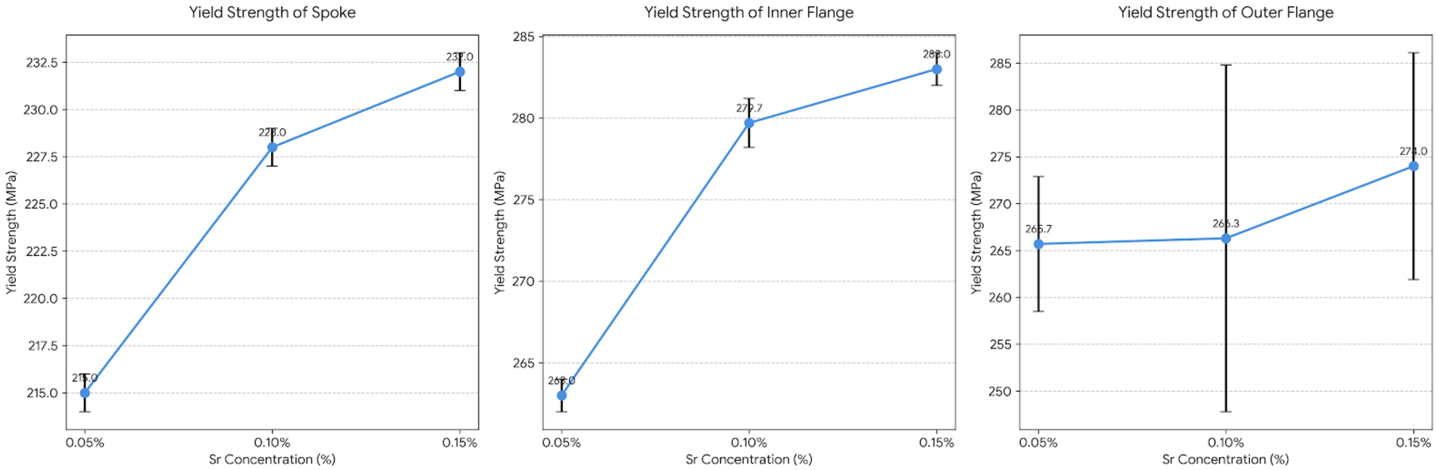

Figure 4. Effect of Sr addition on yield strength of an A356 alloy for spoke, inner flange and outer flange.

3.3. Effect of TiB

Grain-refining additives exert a significant influence on the mechanical properties of cast components. This effect is clearly demonstrated through the comparison of unrefined and refined microstructures shown in Figure 5.

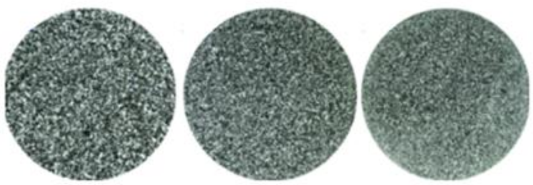

Figure 5. Microstructure of unrefined and refined A356 alloy as a result of TiB addition.

In Figure 5(a), the unrefined microstructure reveals the formation of elongated, wing-like aluminum grains. Brittle intermetallic compounds and porosity regions located between these large grains compromise the material's ductility, especially under stress applied perpendicular to the grain orientation. On the other hand, Figure 5(b) demonstrates a refined microstructure containing small, uniform, and equiaxed grains. This further reinforces the positive effects of TiB in A356 alloys by enhancing overall strength and reliability.

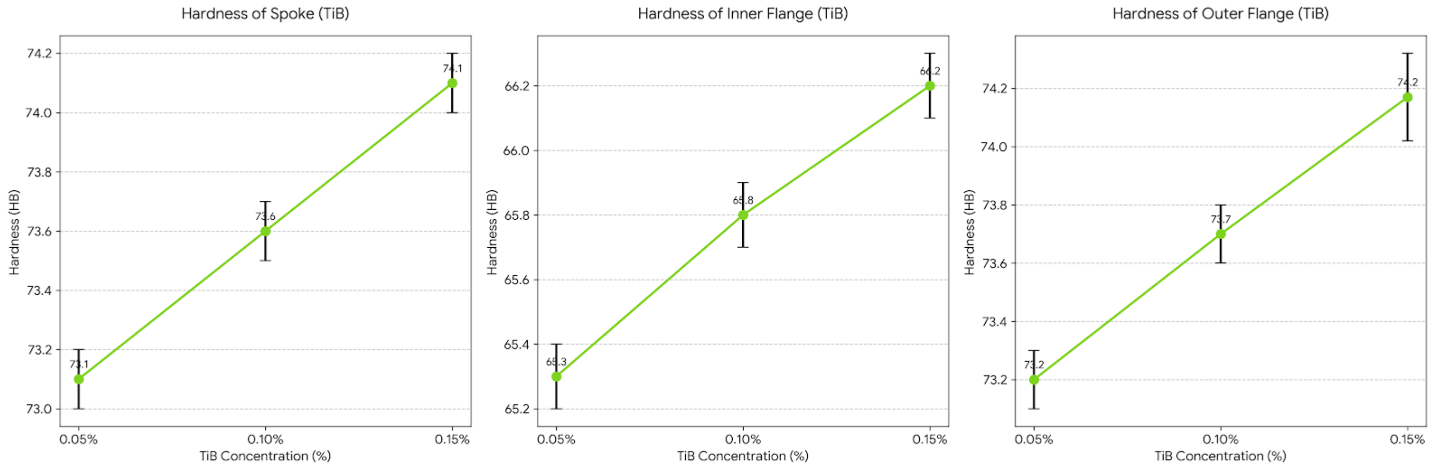

Figure 6. Effect of TiB addition on hardness of an A356 alloy for spoke, inner flange and outer flange.

The three critical regions were assessed for their hardness values with the addition of TiB. All three areas showed an increasing trend in Brinell hardness (HB) as TiB concentration rose from 0.05 wt.% to 0.15 wt.%. The spoke region displayed a gradual but consistent increase in hardness, rising from 73.1 HB at 0.05% TiB to 74.1 HB at 0.15% TiB. Similarly, the outer flange showed improved hardness values, increasing from 73.2 HB to 74.2 HB. Although the inner flange started with a lower base hardness of approximately 65.3 HB, it followed the same trend, reaching its peak hardness of about 66.2 HB at 0.15% TiB.

The increase in hardness is likely due to the formation of a finer microstructure. As described by the Hall-Petch relationship, finer grains result in an increased density of grain boundaries, which act as barriers to dislocation motion, thereby strengthening the material. Standard deviations were notably low (< 0.15 HB), indicating high microstructural uniformity and consistent mechanical performance across all samples.

3.4. Effect of Cu

The addition of copper (Cu) to the A356 alloy resulted in improvements in tensile strength, yield strength, and wear resistance. However, excessive Cu content caused increased brittleness and a higher susceptibility to cracking due to the formation of larger intermetallic phases. Copper addition also promoted precipitation and aging reactions, resulting in a denser and more thermally stable microstructure. Nevertheless, excessive accumulation of Cu was associated with elevated risks of brittleness and corrosion, underscoring the importance of precise compositional control.

4. Conclusion

This research examined the influence of magnesium (Mg), strontium (Sr), titanium boride (TiB), and lastly copper (Cu) additions on the microstructural evolution and mechanical properties of A356 aluminum wheel components produced by low-pressure casting.

Key findings:

- **Magnesium (Mg)**
  - Mg additions resulted in solid solution strengthening and the formation of Mg_2Si precipitates. These precipitates increased Brinell hardness across all regions.
  - The hardness improvements observed were in the range of approximately 10-15 HB as Mg content increased.
  - A reduction in ductility was observed for the spoke and outer flange regions as Mg levels increased.
  - The inner flange revealed a sensitivity to the Mg content as its ductility improved slightly for 0.10% Mg, followed by a decline at 0.15% Mg.
- **Strontium (Sr)**
  - Sr modified the eutectic Si morphology from coarse, acicular structures to a more spheroidized form.
  - Yield strength in the inner flange region increased from approximately 264 MPa to 284 MPa with rising Sr concentration.
  - The microstructural refinement associated with Sr resulted in improved uniformity and enhanced mechanical response.
- **Titanium Boride (TiB)**
  - With the additions of 0.5-0.15% TiB, the microstructure produced finer equaxied.
  - Yield strength imrpovements were typically +3 to +5 Mpa across regions.

- **Copper (Cu)**
  - Both tensile and yield strength were increased due to precipitation hardening.
  - Strength improvements ranged from ~+5 to +10 MPa.

Conflict of Interest

Authors declare that they have no conflict of interest.

References

Aguirre-De la Torre, E., Pérez-Bustamante, R., Camarillo-Cisneros, J., Gómez-Esparza, C. D., Medrano-Prieto, H. M., & Martínez-Sánchez, R. (2013). Mechanical properties of the A356 aluminum alloy modified with La/Ce. *Journal of Rare Earths*, *31*(8), 811-816. https://doi.org/10.1016/S1002-0721(12)60363-9

Cáceres, C. H., & Rovera, D. M. (2001). Solid solution strengthening in concentrated Mg–Al alloys. *Journal of Light Metals*, *1*(3), 151-156. https://doi.org/10.1016/S1471-5317(01)00008-6

Chowwanonthapunya, T., & Peeratatsuwan, C. (2019). Grain refining effect of Al 5Ti 1B master alloy on microstructures and mechanical properties of A356 alloy. *Key Engineering Materials*, *803*, 17-21. https://doi.org/10.4028/www.scientific.net/KEM.803.17

Colak, M., Findik, F., & Yetgin, S. H. (2016). Investigation of the effect of adding Cu on Al alloys for wear and friction properties. *International Journal of Research in Engineering and Technology*, *5*(7), 448-453.

Deepak, G. D., Kashimat, N., Manjunathaiah, K. B., Nayak, V., Anne, G., & Sharma, S. (2025). Optimizing the tribological performance of copper-reinforced A356 aluminum alloy: Influence of heat treatment and composition variation. *Journal of Composites Science*, *9*(6), 287. https://doi.org/10.3390/jcs9060287

Do Lee, C. (2007). Effects of microporosity on tensile properties of A356 aluminum alloy. *Materials Science and Engineering: A*, *464*(1-2), 249-254. https://doi.org/10.1016/j.msea.2007.01.130

Gandin, C. A. (2000). Modeling of microstructure formation in solidification processes. *Iron and Steel Institute of Japan International*, *40*, 971.

Gowri, S., & Samuel, F. H. (1994). Influence of aging and solution treatment on the tensile properties of Al–Si–Cu–Mg cast alloys. *Metallurgical and Materials Transactions A*, *25A*, 437-448.

Kashimat, N., Sharma, S., Nayak, R., Manjunathaiah, K. B., Shettar, M., & Chennegowda, G. M. (2023). Experimental investigation of mechanical property and wear behaviour of T6 treated A356 alloy with minor addition of copper and zinc. *Journal of Composites Science*, *7*(4), 149. https://doi.org/10.3390/jcs7040149

Kashyap, K. T., Murali, S., & Murthy, K. S. S. (1993). Structure and properties of aluminum grain refined with Al–Ti–B. *Materials Science and Technology*, *9*, 189-203.

Kori, S. A., Murty, B. S., & Chakraborty, M. (2000). Influence of grain refiners and modifiers on eutectic nucleation and formation in Al–Si alloys. *Materials Science and Engineering: A*, *283*, 94-104.

Musfirah, A. H., & Jaharah, A. G. (2012). Magnesium and aluminum alloys in automotive industry. *Journal of Applied Sciences Research*, *8*(9), 4865-4875.

Nnakwo, K. C., Nwajioke, C. T., Chukwuneke, J. L., Ugwuanyi, B. C., Ogbunaoffor, K. C., & Ozoh, C. C. (2024). Microstructure evolution in A356 alloy subjected to controlled heat treatment regimes processes. *Discover Applied Sciences*, *6*, Article 497. https://doi.org/10.1007/s42452-024-06143-2

Pramod, S. L., Ravikirana, R., Prasada Rao, A. K., Murty, B. S., & Bakshi, S. R. (2019). Microstructure and mechanical properties of as-cast and T6 treated Sc modified A356-5TiB_2 in-situ composite. *Materials Science and Engineering: A*, *739*, 383-394. https://doi.org/10.1016/j.msea.2018.10.080

Shabestari, S. G., & Moemeni, H. (2004). Effect of copper and solidification conditions on the microstructure and mechanical properties of Al–Si–Mg alloys. *Journal of Materials Processing Technology*, *153-154*, 193-198. https://doi.org/10.1016/j.jmatprotec.2004.04.302

Stojanovic, B., Bukvic, M., & Epler, I. (2018). Application of aluminum and aluminum alloys in engineering. *Advanced Engineering Letters*, *3*(2), Article 2. https://doi.org/10.18485/aeletters.2018.3.2.2

Tash, M., Samuel, F. H., Mucciardi, F., Doty, H. W., & Valtierra, S. (2006). Effect of metallurgical parameters on the machinability of heat-treated 356 and 319 aluminum alloys. *Materials Science and Engineering: A*, *434*(1-2), 207-217. https://doi.org/10.1016/j.msea.2006.06.129

Veldman, N. L. M., Dahle, A. K., StJohn, D. H., & Arnberg, L. (2001). Effect of grain refiner fading on equiaxed zone formation in aluminum alloys. *Metallurgical and Materials Transactions A*, *32A*, 147-155.

Wang, Q. G., & Davidson, C. J. (2001). The influence of porosity on the fatigue life of A356-T6 aluminum alloy. *Journal of Materials Science*, *36*, 739-750.

Xu, M., Ding, W.-W., Hu, L.-W., Chen, S.-H., Zhang, H.-X., Yu, H.-C., & Zhao, W.-J. (2024). Effects of a novel refiner Al-3Ti-4.35La combined with Sr on microstructure and mechanical properties of as-cast A356 alloy. *China Foundry*, *21*, 641-650. https://doi.org/10.1007/s41230-024-3063-4

Yan, W., Fu, G., Xu, Y., Lai, W., & Chen, H. (2021). Effect of Sr addition on the microstructure and properties of the

A356 Al alloy. *Materiali in Tehnologije*, *55*(3), 443. https://doi.org/10.17222/mit.2020.038

Yang, Z. S., Dong, Y., Li, W., & Liu, X. (2022). Strengthening mechanism of Sr element on 6063 Al alloys. *Materials Research Express*, *9*(4), 046501. https://doi.org/10.1088/2053-1591/ac60e4

Zhang, S., Yi, W., Zhong, J., Gao, J., Lu, Z., & Zhang, L. (2023). Computer alloy design of Ti-modified Al-Si-Mg-Sr casting alloys for achieving simultaneous enhancement in strength and ductility. *Materials*, *16*(1), 306. https://doi.org/10.3390/ma16010306

Zhang, Y., & Sills, R. B. (2023). Strengthening via Orowan looping of misfitting plate-like precipitates. *Journal of the Mechanics and Physics of Solids*, *173*, 105234. https://doi.org/10.1016/j.jmps.2023.105234